IL NUOVO CIMENTO Vol. 36 C, N. 1 Suppl. 1 Gennaio-Febbraio 2013
DOI 10.1393/ncc/i2013-11489-2

Colloquia: 12th Italian-Korean Symposium 2011

Oscillating instanton solutions and classification of vacuum bubbles

Bum-Hoon Lee(1)(2)(*), Chul H. Lee(3)(**), Wonwoo Lee(1)(***) and Changheon Oh(3)(**)

(1) *Center for Quantum Spacetime, Sogang University - Seoul 121-742, Korea*
(2) *Department of Physics and BK21 Division, Sogang University - Seoul 121-742, Korea*
(3) *Department of Physics, Hanyang University - Seoul 133-791, Korea*

ricevuto il 9 Marzo 2012

Summary. — We discuss the nucleation process of an oscillating instanton solution and a vacuum bubble in this presentation. We show that there exist the $O(4)$-symmetric oscillating instanton solution and the vacuum bubbles with arbitrary energies. The nontrivial solution corresponding to the tunneling is possible only when gravity is switched on. The geometry of these solutions is finite and preserves the Z_2 symmetry. The action for the solutions are integrable both in de Sitter and in flat background. The instatons do not have any singularity. Our solutions can be interpreted as solutions describing an instanton-induced domain wall or braneworld-like object rather than a kink-induced domain wall or braneworld. The oscillating instanton solutions have a thick wall and the solutions can be interpreted as a mechanism providing nucleation of the thick wall for topological inflation.

PACS 04.62.+v – Quantum fields in curved spacetime.
PACS 98.80.Cq – Particle-theory and field-theory models of the early Universe (including cosmic pancakes, cosmic strings, chaotic phenomena, inflationary universe, etc.).

1. – Introduction

The eternal inflationary universe scenario [1, 2] or multiverse scenario is related to an expanding sea of metastable vacuum, which is also related to the question: How the universe began if it had a beginning? The inflationary universe scenario is seen as a hope

(*) E-mail: bhl@sogang.ac.kr
(**) E-mail: chulhoon@hanyang.ac.kr
(***) E-mail: warrior@sogang.ac.kr
(**) E-mail: och0423@hanyang.ac.kr

for a universe without a beginning. Another scenario as the string theory landscape [3] has many stable and metastable vacua. Hence it is natural to question which vacuum state is related to our universe, even we do not know on the vacuum selection principle that singles out our universe in the landscape. These scenarios seem to provide with escaping from the question on the initial conditions of the universe, *i.e.* it seems to be eternal into the past. Unfortunately, inflationary spacetimes cannot be complete in the past direction [4], even if the universe is eternal into the future. Accordingly, we have a question again. How did the lower vacuum state representing flat or anti-de Sitter background get up the higher vacuum state corresponding to de Sitter background? Can we get a mechanism for the de Sitter universe with some entropy from the state with zero or a very low entropy in an initial causal patch? One may consider another approach which is related to the creation of our universe from nothing by a quantum tunneling [1,5].

With these questions we study the oscillating instanton solutions and classify the possible types of a vacuum bubble, even if the nucleation process of a vacuum bubble becomes only a simple toy model.

The tunneling process is quantum mechanically described by the Euclidean solution obeying appropriate boundary conditions. The Euclidean solution interpolates between two different classical vacua. There exist two kinds of Euclidean solutions describing tunneling phenomena in the double-well potential. One, which is for tunneling in an asymmetric double-well potential, corresponds to a bounce solution. The bounce solution describes the decay of a background vacuum state. The other, which is for tunneling in a symmetric double-well potential, corresponds to an instanton solution.

The bounce solution is related to the nucleation of a true (false) vacuum bubble describing decay of a background vacuum state. The process has been studied within various contexts for several decades. It was fist investigated in ref. [6], developed in flat spacetime and the dynamics was introduced in ref. [7], and developed in the curved spacetime in ref. [8]. This results was enlarged by Parke to the cases with an arbitrary vacuum energy [9]. As a special case of the true vacuum bubble, a vacuum bubble with a finite-sized background after nucleation was studied in ref. [10]. The decay of false monopoles with a gauge group was also studied using the thin-wall approximation [11].

The mechanism for nucleation of a false vacuum bubble in a true vacuum background has also been studied within various contexts. Nucleation of a large false vacuum bubble in dS space was obtained in ref. [12] and nucleation with a global monopole in ref. [13]. The mechanism for nucleation of a small false vacuum bubble was obtained in the Einstein gravity with a nonminimally coupled scalar field [14], with Gauss-Bonnet term in ref. [15], and using Brans-Dicke type theory [16]. The classification of vacuum bubbles including false vacuum bubbles in the dS background in the Einstein gravity was obtained in ref. [17], in which the transition rate and the size of the instanton solution were evaluated in the space, as the limiting case of large true vacuum bubble or large false vacuum bubble. A homogeneous Euclidean configuration in which the scalar field jumps simultaneously onto the top of the potential barrier was investigated in ref. [18]

The oscillating solution with $O(4)$ symmetry in dS space was first studied in ref. [19], where the authors found the solution to oscillating scalar field Φ in fixed background. They adopted the fact that the role of damping term in the particle analogy picture can be changed into that of anti-damping term in dS space if the evolution parameter exceeds half of a given range. The oscillation means that the field in their solutions oscillates back and forth between the two sides of the potential barrier. The analytic computation as the solution of a self-gravitating scalar field and meanings of this type of solution were further studied in ref. [20], in which we have observed that the interpolating solutions are

possible even in AdS space if the local maximum value of the potential is positive. The present work is the study whether there exist oscillating solutions not only in dS but also in both flat and AdS space if the local maximum value of the potential is positive [21].

The paper is organized as follows: in the next section we set up the basic framework for this work. In sect. **2**, we present numerical oscillating instanton solutions by solving the coupled equations for the metric and the scalar field simultaneously. We concentrated on the case in flat background. The case in dS background was emphasized in ref. [21]. In sect. **3**, we classify the possible types of a vacuum bubble in the background with arbitrary vacuum energies. In sect. **4**, we summarize and discuss our results.

2. – Oscillating instanton solutions

The vacuum-to-vacuum transition amplitude can be semiclassically represented as $Ae^{-\Delta S}$, where the exponent ΔS is the difference between the Euclidean action corresponding to a classical solution and the background action itself. The pre-factor A comes from the first-order quantum correction.

We consider the following action:

$$S = \int_{\mathcal{M}} \sqrt{-g}\mathrm{d}^4x \left[\frac{R}{2\kappa} - \frac{1}{2}\nabla^\alpha\Phi\nabla_\alpha\Phi - U(\Phi)\right] + \oint_{\partial\mathcal{M}} \sqrt{-h}\,\mathrm{d}^3x \frac{K-K_o}{\kappa}\,, \tag{1}$$

where $g \equiv \det g_{\mu\nu}$, $\kappa \equiv 8\pi G$, R denotes the scalar curvature of the spacetime $\mathcal{M}$, K and K_o are the traces of the extrinsic curvatures of $\partial\mathcal{M}$ in the metric $g_{\mu\nu}$ and $\eta_{\mu\nu}$, respectively, and the second term on the right-hand side is the boundary term [22]. The gravitational field equations can be obtained properly from a variational principle with this boundary term. This term is also necessary to obtain the correct action.

The potential $U(\Phi)$, which represents the energy density of a homogeneous and static scalar field, has two degenerate minima

$$U(\Phi) = \frac{\lambda}{8}\left(\Phi^2 - \frac{\mu^2}{\lambda}\right)^2 + U_0. \tag{2}$$

The cosmological constant is given by $\Lambda = \kappa U_o$, hence the space will be dS, flat, or AdS depending on whether $U_0 > 0$, $U_0 = 0$, or $U_0 < 0$.

To evaluate ΔS and show the existence of the solution, one has to take the analytic continuation to Euclidean space. We assume the $O(4)$ symmetry for both the geometry and the scalar field as in ref. [8]

$$\mathrm{d}s^2 = \mathrm{d}\eta^2 + \rho^2(\eta)\left[\mathrm{d}\chi^2 + \sin^2\chi\left(\mathrm{d}\theta^2 + \sin^2\theta\mathrm{d}\phi^2\right)\right]. \tag{3}$$

In this case Φ and ρ depend only on η, and the Euclidean field equations for them can be written in the form:

$$\Phi'' + \frac{3\rho'}{\rho}\Phi' = \frac{\mathrm{d}U}{\mathrm{d}\Phi} \qquad \text{and} \qquad \rho'' = -\frac{\kappa}{3}\rho(\Phi'^2 + U), \tag{4}$$

respectively and the Hamiltonian constraint is given by

$$\rho'^2 - 1 - \frac{\kappa\rho^2}{3}\left(\frac{1}{2}\Phi'^2 - U\right) = 0. \tag{5}$$

In order to yield the solution the constraint requires a delicate balance among the terms. Otherwise the solution can provide qualitatively incorrect behavior [23].

For this to work, we choose the values of the field ρ and derivatives of the field Φ as follows:

$$\rho|_{\eta=0} = 0, \qquad \rho|_{\eta=\eta_{max}} = 0, \qquad \left.\frac{\mathrm{d}\Phi}{\mathrm{d}\eta}\right|_{\eta=0} = 0, \qquad \text{and} \qquad \left.\frac{\mathrm{d}\Phi}{\mathrm{d}\eta}\right|_{\eta=\eta_{max}} = 0, \tag{6}$$

where η_{max} is the maximum value of η and will have a finite value. These conditions are useful for obtaining solutions with Z_2 symmetry.

To simplify things, we only consider the Euclidean action of the bulk part in eq. (1) to get,

$$S_E = \int_{\mathcal{M}} \sqrt{g_E}\, \mathrm{d}^4x_E \left[-\frac{R_E}{2\kappa} + \frac{1}{2}\Phi'^2 + U\right] = 2\pi^2 \int \rho^3 \mathrm{d}\eta[-U], \tag{7}$$

where $R_E = 6[1/\rho^2 - \rho'^2/\rho^2 - \rho''/\rho]$ and we used eqs. (4) and (5) to arrive at this. Thus the contributions coming from the geometry and kinetic energy in the Euclidean action are included to be the potential effectively. The volume energy density has the following form:

$$\xi \equiv -\mathcal{H} = -\left[-\frac{R_E}{2\kappa} + \frac{1}{2}\Phi'^2 + U\right] = U. \tag{8}$$

We will examine the change in the density with respect to the evolution parameter η.

In the thin-wall approximation scheme, the Euclidean action can be divided into three parts: $\Delta S = \Delta S_{in} + \Delta S_{wall} + \Delta S_{out}$, where $\Delta S = S_E(\text{solution}) - S_E(\text{background})$. The contribution from the wall is $\Delta S_{wall} = 2\pi^2 \bar{\rho}^3 S_o$, where the surface tension of the wall $S_o(= 2\mu^3/3\lambda)$ is a constant, *i.e.* the uniform tension having the same value at all pints on the surface. In the wall, the scalar field varies continuously between the true and false vacuum values. If the thickness of the wall is small compared to the radius of the wall, we can use the thin-wall approximation.

Actually, the wall can be a source of repulsive gravitation ($p < 0$), unlike the usual pressure ($p > 0$) representing a source of gravitational attraction.

In ref. [21], we have considered oscillating instanton solutions in dS background, in the main. In this work, we consider mainly the solutions in flat background.

Figure 1 shows oscillating instanton solutions representing tunneling starting from left vacuum state in the case of flat-flat degenerate vacua. We take dimensionless variable [20] $\tilde{\kappa} = 0.2$ for all the cases. The first figure illustrates the potential, in which the number n denotes the number of the crossing or the number of oscillations. The maximum number n_{max} is 6. The second figure illustrates the initial point $\tilde{\Phi}_o$ for each number of oscillations. As expected, the number of oscillations increases as the initial point, $\tilde{\Phi}(\tilde{\eta}_{initial}) = \tilde{\Phi}_o$, moves away from the vacuum state. The third figure illustrates the solutions of $\tilde{\rho}$. We can see that the size of the geometry with a solution decreases as the number of crossing increases because the period of the evolution parameter $\tilde{\eta}_{max}$ decreases as the starting point moves away from the vacuum state. The solution of $\tilde{\rho}$ is $\tilde{\eta}$ in fixed flat space. Thus, the straight evolution line of $\tilde{\rho}$ near the vacuum state indicate flat space. Figure 1(i) illustrates the one-crossing solution, $n = 1$, of the field $\tilde{\Phi}$. Figure 1(ii) illustrates the two-crossing solution, $n = 2$. There does not exist this

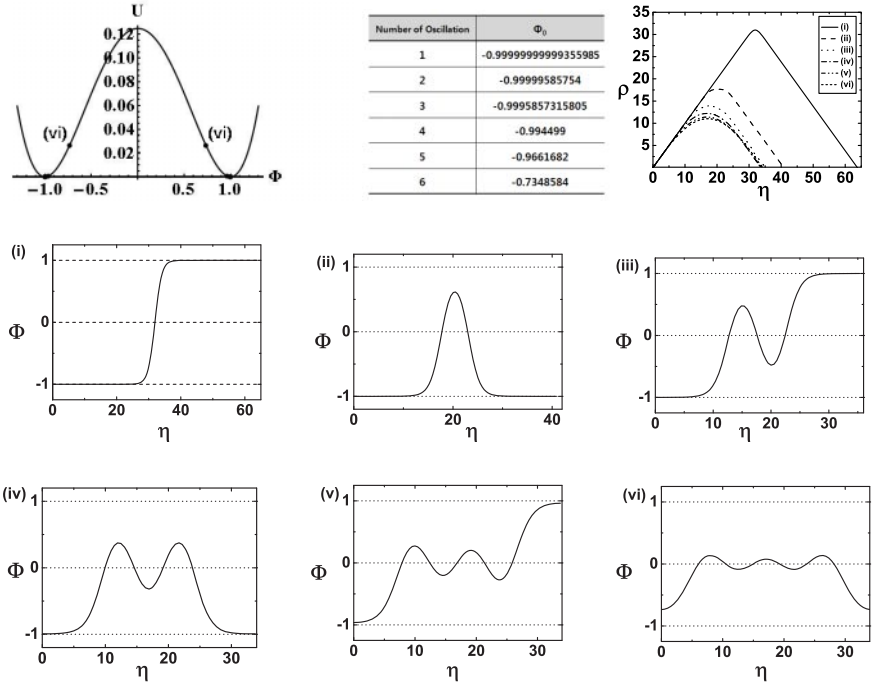

Fig. 1. – The numerical solutions represent oscillating instanton solutions between flat-flat degenerate vacua.

type of the solution including bounce solutions when gravity is switched off. However, the solution is somewhat different from the double-bounce solution in ref. [24]. Since our solution of $\tilde{\Phi}$ does not asymptotically approach the other vacuum state, it is difficult that we interpret our solution as the double-instanton solution or the spontaneous pair-creation of instanton solutions. Figures 1(iii)-(vi) illustrate the n-crossing solution, $n = 3, 4, 5, 6$. Figures 1(i), (iii), and (v) illustrate the tunneling starting from the left vacuum state to the right vacuum state. Figures 1(ii), (iv), and (vi) illustrate solutions going back to the starting point after oscillations. This type of solutions is possible only if gravity is taken into account. The maximum number of oscillations is determined by the parameters $\tilde{\kappa}$ and $\tilde{U}_o$ observed in ref. [19].

Figure 2 shows the variation of terms, $\tilde{\rho}'$, $\tilde{\Phi}'$, $\tilde{\rho}''$, $\frac{3\tilde{\rho}'}{\tilde{\rho}}\tilde{\Phi}'$, and $\mathrm{d}\tilde{U}/\mathrm{d}\tilde{\Phi}$, with respect to $\tilde{\eta}$ in eqs. (4) and (5). In figs. 1(i)-(vi), we see that the sign change of $\tilde{\rho}'$ from positive to negative occurs at the half period due to the Z_2 symmetry. The value of $\tilde{\rho}'$ at near initial and final value of $\tilde{\eta}$ means the flat space at that point. The value of ρ' spans from 1 to -1 in all figures. The transition region of $\tilde{\rho}'$ means the rolling duration in the inverted potential. In that region, all other terms also have dynamical behavior. The value of $\tilde{\Phi}''$ representing an acceleration of the particle in the inverted potential increases, decreases, and becomes zero at the half period. The graph is odd function. The value of $\tilde{\rho}''$ is always negative or zero as an even function according to eq. (4). The damping term also increases, decreases, and becomes zero as an odd function. The term $\mathrm{d}\tilde{U}/\mathrm{d}\tilde{\Phi}$ has got the same property. Figures 2(i), (iii), and (v) representing tunneling show that $\tilde{\rho}'$, $\tilde{\Phi}''$, damping term, and $\mathrm{d}\tilde{U}/\mathrm{d}\tilde{\Phi}$ change their sign simultaneously at the half period. While

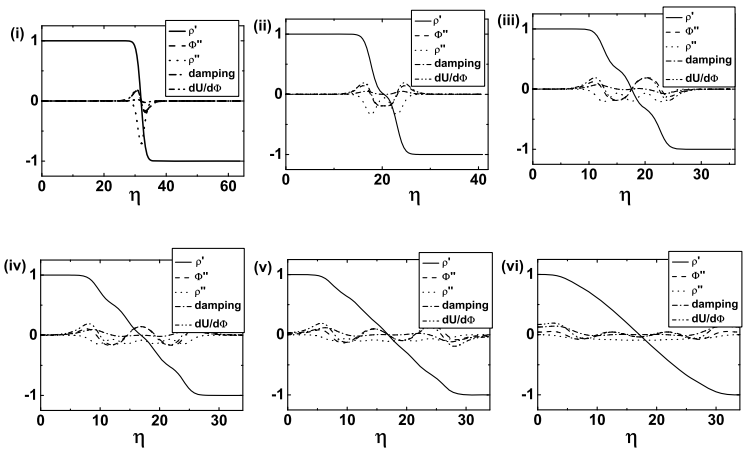

Fig. 2. – Variation of terms in equations of motion between flat-flat degenerate vacua.

figs. 2(ii), (iv), and (iv) representing solutions going back to the starting point show that only $\tilde{\rho}'$ change its sign at the half period. All of the behaviors represented in each figure can be well understood bearing Z_2 symmetry in mind.

The behavior of the solutions in the $\tilde{\Phi}(\tilde{\eta})$-$\tilde{\Phi}'(\tilde{\eta})$ plane using the phase diagram method is shown in fig. 3. Figure 3(i) illustrates the phase diagram of a one-crossing solution, in which the trajectory is restricted to the upper half region in the diagram. It is the turning point from the damping phase to the anti-damping phase when $\tilde{\Phi}'$ is the maximum value and $\tilde{\Phi}$ attains the first zero. The value of $\tilde{\Phi}$ spans from -1 to $+1$ and $\tilde{\Phi}'$ from zero via maximum value to ~ 0.49, to zero with symmetry about the y-axis. Figure 3(ii) illustrates the diagram of a two-crossing solution, in which the trajectory does not reach the opposite point $\tilde{\Phi} = 1$ but return to the starting point $\tilde{\Phi} = -1$. When the trajectory goes back, $\tilde{\Phi}'$ is negative with symmetry about the x-axis. It is the turning point from the damping phase to the anti-damping phase when $\tilde{\Phi}'$ reaches the second zero and $\tilde{\Phi}$

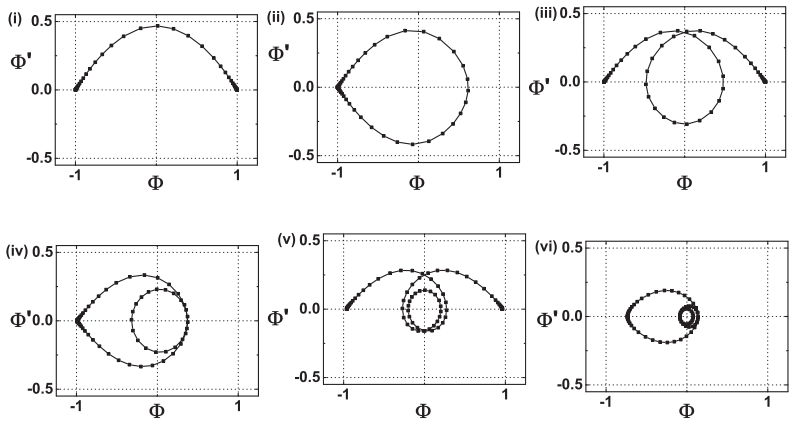

Fig. 3. – The behavior of the solutions in the Φ-Φ' plane using the phase diagram method. The case is belong to the tunneling between flat-flat degenerate vacua.

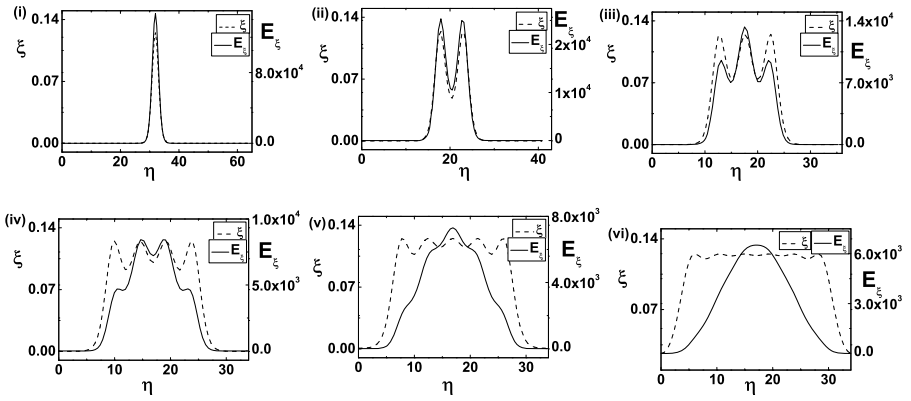

Fig. 4. – The diagram of energy density of each solutions. In each figure, the dotted line denotes the volume energy density ξ and the solid line denotes the Euclidean energy E_ξ at constant η.

takes positive value. Figure 3(iii) illustrates the diagram of three-crossing solution. It is the turning point when $\tilde{\Phi}'$ takes the negative maximum value and $\tilde{\Phi}$ attains the second zero. Figure 3(iv) illustrates the diagram of four-crossing solution. It is the turning point when $\tilde{\Phi}'$ reaches the third zero and $\tilde{\Phi}$ takes negative value. The figure (v) illustrates the diagram of five-crossing solution. It is the turning point when $\tilde{\Phi}'$ takes the positive value and $\tilde{\Phi}$ attains the second zero. Figure 3(vi) illustrates the diagram of six-crossing solution. It is the turning point when $\tilde{\Phi}'$ reaches the third zero and $\tilde{\Phi}$ takes the positive value. Figures 3(i), (iii), and (v) have symmetry about the y-axis, whereas (ii), (iv), and (vi) have symmetry about the x-axis. The maximum value of $\tilde{\Phi}'$ decreases as the number of crossing increases.

Figure 4 shows the diagram of the energy density of each solutions. In each figure, the solid line denotes the Euclidean energy E_ξ and the dotted line denotes the volume energy density ξ in eq. (8). The Euclidean energy signifies the value after the integration of variables except for η in the present work. The peaks represent a rolling phase in the valley of the inverted potential. The maximum value ξ_{max} is equivalent to U_{top}. The number of peaks is thus equal to the number of crossing. The peaks broaden in their range near U_{top} as the number of crossing increases. The Euclidean energy also has peaks. However, the shape of the peaks becomes smooth and broadens as the number of crossing increases. As can be seen from fig. 4(vi), the thickness of the wall increases as the number of oscillations increases.

3. – Classification of vacuum bubbles

In this section, we consider the following potential:

$$U(\Phi) = \frac{\lambda}{8}\left(\Phi^2 - \frac{\mu^2}{\lambda}\right)^2 - \frac{\epsilon\sqrt{\lambda}}{2\mu}\left(\Phi - \frac{\mu}{\sqrt{\lambda}}\right) + U_o, \tag{9}$$

where $U(\Phi)$ has two non-degenerate minima with lower minima at Φ_T and higher minima at Φ_F. The parameter ϵ represents the energy-density difference between $U(\Phi_F)$ and $U(\Phi_T)$.

We first classify the true vacuum bubbles according to the ref. [17], in which vacuum bubbles were classified in a de Sitter background. We extend the possible type of true vacuum bubbles to the cases including finite flat and anti-de Sitter background [25].

Now we consider the contribution from $\Delta S_{in} = S_E^{in}(\text{solution}) - S_E^{in}(\text{background})$. For the general expression

$$S_E^{in}(\text{solution}) = 4\pi^2 \left[\int_0^{\rho_{max}} \mathrm{d}\rho \frac{\rho^3 U_T - \frac{3\rho}{\kappa}}{(1-\frac{\kappa}{3}\rho^2 U_T)^{1/2}} - \int_{\rho_{max}}^{\bar{\rho}} \mathrm{d}\rho \frac{\rho^3 U_T - \frac{3\rho}{\kappa}}{(1-\frac{\kappa}{3}\rho^2 U_T)^{1/2}} \right], \tag{10}$$

$$S_E^{in}(\text{background}) = 4\pi^2 \left[\int_0^{\rho_{max}} \mathrm{d}\rho \frac{\rho^3 U_F - \frac{3\rho}{\kappa}}{(1-\frac{\kappa}{3}\rho^2 U_F)^{1/2}} - \int_{\rho_{max}}^{\bar{\rho}} \mathrm{d}\rho \frac{\rho^3 U_F - \frac{3\rho}{\kappa}}{(1-\frac{\kappa}{3}\rho^2 U_F)^{1/2}} \right],$$

where $\rho_{max}(F/T) = \sqrt{3/\kappa U_{F/T}}$ for dS geometry. This can be seen by the relation

$$\mathrm{d}\rho = \pm \mathrm{d}\eta \left[1 - \frac{\kappa \rho^2 U}{3} \right]^{1/2}, \tag{11}$$

where + for $0 \le \eta < \eta_{max}/2$, 0 for $\eta = \eta_{max}/2$, and − for $\eta_{max}/2 < \eta \le \eta_{max}$.

For a true vacuum bubble, the contribution from the outside ΔS_{out} will be zero since the outside geometry will be not changed after the nucleation. However, if one consider the cases including finite flat and anti-de Sitter background one should consider the effect. The contribution from the outside the wall is vanishing for dS, on the other hand the contribution is non-vanishing for flat and AdS space. The final form from the contribution of the outside part in both flat and AdS space is evaluated to be

$$B_{out} = \frac{12\pi^2}{\kappa^2 U_F} \left[2 \left(1 - \frac{\kappa}{3} \bar{\rho}^2 U_F \right)^{3/2} \right] + B_{feff}, \tag{12}$$

where $B_{feff} = -\frac{12\pi^2}{\kappa^2 U_F}[1 + (1 - \frac{\kappa}{3}\tilde{\rho}^{i2}_{max} U_F)^{3/2}] + B_{ibp}$ and where the second term in the right-hand side of the above equation is from the effect of the surface term at $\tilde{\rho}^i_{max}$ and $\Delta S_{ibp} = -(6\pi^2/\kappa)\tilde{\rho}^{i2}_{max}(1 - \kappa\tilde{\rho}^{i2}_{max} U_F/3)^{1/2}$. For dS space, $\rho^i_{max}(\eta_{max}) = 0$ and $\Delta S_{ibp} = 0$.

In the present proceedings, we shall be simply presenting the possibly types of a vacuum bubble.

- The types of true vacuum bubbles [17, 25]: 1) flat bubble - large dS background, 2) flat bubble - half dS background, 3) flat bubble - small dS background, 4) AdS bubble - large dS background, 5) AdS bubble - flat dS background, 6) AdS bubble - small dS background, 7) dS small bubble - large dS background, 8) dS small bubble - flat dS background, 9) dS small bubble - small dS background, 10) AdS bubble - flat infinite background, 11) AdS bubble - AdS infinite background, 12) AdS bubble - flat finite background, 13) AdS bubble - AdS infinite background.

- The types of false vacuum bubbles [25]: 1) dS large bubble - dS small background, 2) dS half bubble - dS small background, 3) dS small bubble - dS small background, 4) dS large bubble - flat finite background, 5) dS half bubble - flat finite background, 6) dS small bubble - flat finite background, 7) dS large bubble - AdS

finite background, 8) dS half bubble - AdS finite background, 9) dS small bubble - AdS finite background, 10) flat bubble - AdS finite background, 11) AdS bubble - AdS finite background.

4. – Summary and discussions

In this presentation, we have discussed oscillating instanton solutions of a self-gravitating scalar field between degenerate vacua and possible types of a vacuum bubble.

As a result of this tunneling, a finite-sized geometry with Z_2 symmetry is obtained. Our mechanism for making the domain wall or braneworld-like object is different from the ordinary formation mechanism of the domain wall because our solutions are instanton solutions rather than soliton solutions. In other words, our solutions can be interpreted as solutions describing an instanton-induced domain wall rather than a kink-induced domain wall or braneworld-like object. Domain walls can form in any model having a spontaneously broken discrete symmetry. An inertial observer sees the domain wall accelerating away with a specific acceleration. The thickness of the domain wall in flat spacetime can be estimated by a balance between the potential energy and the gradient energy. When the thickness of the domain wall is greater than or equal to the horizon size corresponding to the vacuum energy in the interior of the domain wall, topological inflation can occur [26]. The scalar field stays near the top of the potential at the core. This potential energy serves as a vacuum energy in a similar way to the slow-rollover inflationary models. This topological inflation does not require fine-tuning of the initial conditions and is eternal even at the classical level due to the topological reason. Our oscillating instanton solutions can be interpreted as mechanism providing the nucleation of the thick wall for the topological inflation, even though we started in the arbitrary vacuum state. The wrinkles representing the variation of the volume energy density in the wall may be interpreted as density perturbations in the inflating region. In this work, inflating regions described by the oscillating solutions and density perturbations described by the variation of energy density can occur simultaneously. Furthermore, oscillating bounce solutions also have the thick wall. Thus we expect that (non-)topological inflation can be made by oscillating bounce solutions.

* * *

We would like to thank Wontae Kim, Hyun Seok Yang, and Dong-han Yeom for helpful discussions and comments. We would like to thank Remo Ruffini, Hyung Won Lee, and She-Sheng Xue for their hospitality at the 12th Italian-Korean Symposium on Relativistic Astrophysics in Pescara, Italy, 4-8 Jul 2011. This work was supported by the Korea Science and Engineering Foundation (KOSEF) grant funded by the Korea government(MEST) through the Center for Quantum Spacetime(CQUeST) of Sogang University with grant number R11 - 2005 - 021. WL was supported by the National Research Foundation of Korea Grant funded by the Korean Government (Ministry of Education, Science and Technology) [NRF-2010-355-C00017].

REFERENCES

[1] Vilenkin A., *Phys. Rev. D*, **27** (1983) 2848.
[2] Linde A. D., *Phys. Lett. B*, **175** (1986) 395; Guth A. H., *Phys. Rep.*, **333-334** (2000) 555; Vilenkin A., preprint [arXiv:gr-qc/0409055].

[3] Bousso R. and Polchinski J., *JHEP*, **06** (2000) 006; Susskind L., preprint [arXiv:hep-th/0302219]; Ashok S. K. and Douglas M., *JHEP*, **01** (2004) 060.
[4] Borde A., Guth A. H. and Vilenkin A., *Phys. Rev. Lett.*, **90** (2003) 151301.
[5] Hartle J. B. and Hawking S. W., *Phys. Rev. D*, **28** (1983) 2960.
[6] Voloshin M. B., Kobzarev I. Yu. and Okun L. B., *Yad. Fiz.*, **20** (1974) 1229 (*Sov. J. Nucl. Phys.*, **20** (1975) 644).
[7] Coleman S. R., *Phys. Rev. D*, **15** (1977) 2929; **16** (1977) 1248(E).
[8] Coleman S. R. and De Luccia F., *Phys. Rev. D*, **21** (1980) 3305.
[9] Parke S., *Phys. Lett. B*, **121** (1983) 313.
[10] Aguirre A., Banks T. and Johnson M., *JHEP*, **08** (2006) 065; Bousso R., Freivogel B. and Lippert M., *Phys. Rev. D*, **74** (2006) 046008.
[11] Kumar B., Paranjape M. B. and Yajnik U. A., *Phys. Rev. D*, **82** (2010) 025022.
[12] Lee K. and Weinberg E. J., *Phys. Rev. D*, **36** (1987) 1088.
[13] Kim Y., Maeda M. and Sakai N., *Nucl. Phys. B*, **481** (1996) 453; Kim Y., Lee S. J., Maeda M. and Sakai N., *Phys. Lett. D*, **452** (1999) 214.
[14] Lee W., Lee B.-H., Lee C. H. and Park C., *Phys. Rev. D*, **74** (2006) 123520.
[15] Cai R. G., Hu B. and Koh S., *Phys. Lett. B*, **671** (2009) 181.
[16] Kim H., Lee B.-H., Lee W., Lee Y. J. and Yeom D.-h., *Phys. Rev. D*, **84** (2011) 023519; Lee B.-H., Lee W. and Yeom D.-h., *J. Cosmol. Astropart. Phys.*, **01** (2011) 005.
[17] Lee B.-H. and Lee W., *Class. Quantum Grav.*, **26** (2009) 225002.
[18] Hawking S. W. and Moss I. G., *Phys. Lett. B*, **110** (1982) 35.
[19] Hackworth J. C. and Weinberg E. J., *Phys. Rev. D*, **71** (2005) 044014.
[20] Lee B.-H., Lee C. H., Lee W. and Oh C., *Phys. Rev. D*, **82** (2010) 024019.
[21] Lee B.-H., Lee C. H., Lee W. and Oh C., preprint [arXiv:1106.5865].
[22] York J. W. Jr., *Phys. Rev. Lett*, **28** (1972) 1082; Gibbons G. W. and Hawking S. W., *Phys. Rev. D*, **15** (1977) 2752; York J. W. Jr., *Found. Phys.*, **16** (1986) 249.
[23] Berger B. K., *Gen. Rel. Grav.*, **38** (2006) 625.
[24] Bousso R. and Linde A., *Phys. Rev. D*, **58** (1998) 083503.
[25] Lee B.-H., Lee C. H., Lee W. and Oh C., in preparation.
[26] Vilenkin A., *Phys. Rev. Lett.*, **72** (1994) 3137; Linde A., *Phys. Lett. B*, **327** (1994) 208.